INTELLIGENT FAULT DIAGNOSIS OF ROBOT BEARING BASED ON MULTI-INFORMATION

Ziyue WU [1,*], Yang LIU[1], Xinxing LI[2], Xingxing DU[3], Bing WANG[1]

Based on the condition assessment of thin-walled robot bearing, a fault diagnosis method based on multi-information fusion is proposed. The vibration data and acoustic emission (AE) data of the thin-walled robot bearing are extracted and constructed a fusion model of multi-feature data; finally, the self-organizing map (SOM) neural network is used to assess the fusion model. With analysis and verification of measured data, the method can assess the fault type of thin-walled robot bearing effectively, and it provides a new reference for condition assessment of thin-walled robot bearing.

Keywords: Robot bearing; Multi-information fusion; Fault diagnosis; Vibration; AE; SOM neural network

1. Introduction

Nowadays, robots have been developing towards being compact and exquisite. As key components of robots, robot bearings' stable and safe operation is determinant to the overall performance of the robot. Therefore, the research on robot bearings is highly valuable both theoretically and practically.

Among all kinds of bearings, thin-walled robot bearing has been highly favored by the robot industry thanks to its unique traits, such as being light, exquisite, and small. And so far, a great number of experts and scholars have researched thoroughly on robot bearings. Cai [1] analyzed the structural design of thin-walled bearings for industrial robots. Wang [2] analyzed and studied how thin-walled bearing rings were positioned in rotating gas fields. Jiang [3] analyzed the deformation, stress and load distribution of the inner and outer rings of flexible bearings while also took pre-deformation, pre-stress and actual load conditions of the inner and outer rings of flexible bearings into consideration. Considering the serious problems during the heat treatment process of thin-walled light series high-precision bearing rings, Jia [4] proposed to reduce the quenching deformation rate of the thin-walled bearing rings by using a semi-automatic

[1] School of Mechanical & Electronic Engineering, Henan University of Science and Technology, Luoyang 471003, Henan, China
[2] Softlink Powered By Googoltech, Luoyang 471003, Henan, China
[3] Googol Technology Limited, Shenzhen 250000, China
* Corresponding author: Ziyue Wu, wuziyuetutu@126.com

quenching press to optimize the quenching mold pressure. In order to accurately obtain the surface circumferential stress distribution and deformation conditions of the bearing rings, Kashif [5] developed a new equalization algorithm, based on Newtonian mechanics. Ostapski [6,7] used the finite element method to analyze the deformation and stress of flexible bearings under the application of a symmetrical radial load in the long axis region. For now, these studies mainly focus on the structure, performance, vibration characteristics, and application prospects of robot bearings. In terms of fault diagnosis, Sui [8] studied the new threshold de-noising method based on stationary wavelet and discussed the fault feature extraction method based on image technology. Based on the detailed discussion of the noise reduction, feature extraction, current research status of compound and intelligent fault diagnosis of rolling bearings, Deng [9] deeply investigated several key issues involved in the feature extraction and diagnosis of rolling bearings faults with regard to the analysis and process method of vibration signals. Taking rolling bearings as research subject, He [10] proposed a kernel function Eigen-matrix combined with approximate diagonalization feature fusion method. Combining with other signal processing methods and machine learning methods, He further investigated feature extraction, fault identification, and performance degradation evaluation of rolling bearings. Xue [11] deeply investigated the AE signals of aero-engine rolling bearings faults and has greatly improved the fault recognition rate. Taking rolling bearings, one of the most common yet critical components of aero-engines, as research subject, after fully studied the vibration mechanism and signal characteristics of rolling bearings and investigated the research status of bearing fault diagnosis both internationally and domestically, Jiang [12] proposed a fault diagnosis method for aero-engine bearings based on texture features. Wang [13] studied the fault diagnosis applications of rolling bearings based on sparsely expressed mechanical signal processing methods. Baillie [14] compared three different autoregressive models, namely linear autoregressive model, Back-Propagation (BP) neural network, radial basis function network, and then applied the three models in bearing fault diagnosis, respectively. Qiu [15] extracted the weak fault features of the bearing under the strong noise interference by optimizing the correlation of Morlet wavelets through the minimum Shannon entropy principle parameters and using the singular value decomposition to select the appropriate wavelet transform scale. Kumar [16] used discrete wavelet transform to detect the outer ring fault size of the tapered roller bearings. Also, he managed to control the error within a small range by using Sytnlet5 wavelet to extract the fault impact information in the signals. Since single sensor identification has certain limitations and is susceptible to the sampling environment, while multi-sensor identification technology has diversified the source of information, increased the fault tolerance of the system, and improved the confidence and reliability of the system, more

and more scholars have conducted research on multi-sensor technology. Han [17] studied the multi-sensor information fusion fault diagnosis method based on time series analysis and stepwise variable prediction model (AR-SVPMCD) technology. Based on Genetic Algorithm- Back Propagation (GA-BP) neural network's multi-sensor information fusion method, Li [18] collected vibration signals of both normal and abnormal operating conditions by building signal acquisition systems and arranging accelerometer sensors around bearings. Han [19] comprehensively discussed collection, feature extraction and feature model construction of both acceleration signals and acoustic emission signals of rolling bearing faults and proposed a multi-information fusion method based on BP neural network. Based on deep belief network and multi-sensor information fusion technology, Yu [20] investigated fault diagnosis methods of rolling bearings. However, the research on multi-sensor is mostly based on AR-SVPMCD technology and BP neural network while few adopted SOM neural network modeling technology for robot bearings. By analyzing two acoustic emission characteristic signal parameters of ringing count and peak value of rolling bearing with three kinds of faults, including inner ring, outer ring and rolling body, Tandoh [21] studied the influence law of bearing structure parameters and operation parameters on ringing count and peak value, and concluded that it is more accurate to identify faults through peak value. Choudhary [22] studied the relationship between faults and characteristic signals of rolling bearings in different periods, and obtained that early faults of bearings can be detected by ringing count and the development direction of faults can be predicted at the same time. Liu [23] used the sparse expression algorithm to optimize the weight matrix of the local linear embedding method, so as to realize the manifold dimension reduction of fault signals that could better reveal the signal characteristics, and optimize the fault diagnosis mode.

SOM neural network is a competitive neural network modeled on the self-organizing mapping function of the human brain system and has a strong classification characteristic for input vectors. Through its continuous learning cycle, the probability distribution of input models and the space distribution density of connection weights tend to be the same. In view of this, based on the SOM neural network, multi-sensor identification technology is used in this paper to investigate robot bearings faults. Firstly, the vibration information and AE information of faults are extracted to construct the multi-characteristic neural network information model. Then, the dimensional and dimensionless parameters are used to realize the fault diagnosis of robot bearings through SOM neural network.

2. State feature parameter selection based on multi-information fusion

Since multi-information fusion technology has the characteristic that multi-sensor measurement results complement each other and is able to diagnose and decide the importance of variables, its information sources are diverse and the possibility of being influenced by environment is rather low.

Among all information fusion technologies, vibration signal detection and AE signal detection are being used most widely. Specifically, vibration signal detection is the most widely used detection method in engineering. But solely using vibration signal to detect faults in the early stages has been failing to provide ideal results since vibration signals are not only insensitive to slight faults in the early stages, but also easily influenced by the surrounding noise signals significantly. However, AE signal, a fault caused by the rapid energy releasing of the component's own structure's part material stress concentration, is known to be almost insusceptible to surrounding environment. Therefore, AE signal has been applied to the fault diagnosis of components in the early stages. Undoubtedly, fusing vibration signals and AE signals will significantly improve the accuracy and sensitivity of fault diagnosis. Thus, this paper extracts the state characteristic parameters of rolling bearings' vibration signals and AE signals.

Generally speaking, there are mainly two kinds of rolling bearings' vibration signals. One is the vibration signal generated by the rolling bearing due to its own structure being under working conditions and is therefore determined by the structure of the bearing itself, and the other is caused by the faults of the rolling bearing's components under the working condition and is able to reflect the form and degree of the bearing's faults. AE signal are usually in three types, namely burst type, continuous type, and a mixed type which combines both signals. But in the actual use, the signals detected are often very complex and tend to be mixed signals. For both vibration signals and AE signals, the most common analytical methods are time domain analysis and frequency domain analysis.

Time domain analysis simply analyzes the collected signal directly on a time axis. The whole process is simple and clear and is therefore easy to see the dynamic situation of the signals in real time. Its characteristic parameters can be divided into dimensional parameters and dimensionless parameters. Dimensional parameters generally include mean value, root mean square value, variance, standard deviation, and peak value. And dimensionless parameters generally include waveform index, peak indexes, pulse index, kurtosis index, and margin index. Taking some parameters as examples, some time domain analyses are shown as follows.

Mean value is the average value of the collected sample signals and therefore is able to reflect the overall trend of the signals. As the faults of bearings evolve, the signal information collected by the sensors also differs, and the mean

value can be used as one of the methods of diagnosing the faults of the rolling bearings.

Mean square value is the average value of the total energy of the collected signals. As the faults of rolling bearings occur, the signals collected by the sensor are no longer stable, and the peak of the interval begins to appear. At this time, the power of the signals will also begin to increase. Therefore, the diagnosis of bearings' faults can also be achieved by monitoring the mean square value of the collected signals.

Autocorrelation function can reflect the degree of similarity between the collected signals and retain the information of the amplitude of the original collected signals. However, the phase information of the collected signals is not indicated in the function. In the formula, T is the total time.

Cross-correlation function can not only retain the amplitude information of the collected signals, but also reflect the phase information of the analyzed signals. The original frequency information can be reflected on the frequency spectrum. Therefore, this method is commonly used when conducting time domain analysis of signals.

Frequency domain analysis analyzes the collected signals in the frequency domain rather than the time domain and can clearly reflect the characteristics of the bearings' faults. Basic frequency domain analysis includes phase spectrum, power spectrum, energy spectral density, coherence function and so forth. Some frequency domain analyses are shown as follows.

Spectrum:

If the time domain signal $x(t)$ satisfies the–Dirichlet condition [24], the mathematical expression of the spectrum function is:

$$X(\omega) = \int_{-\infty}^{+\infty} x(t) e^{-i\omega t} \mathrm{d}t \tag{1}$$

Where, the notation ω represents the angular frequency, i is the imaginary unit.

Phase spectrum can be expressed as a module of the spectral function $X(\omega)$, which is called the amplitude spectrum of $x(t)$.

Power spectrum:

Power spectrum represents the degree of energy distribution of the collected signals in the frequency domain. Its mathematical expression is:

$$S_x(\omega) = \left|F(\omega)\right|^2 = \int_{-\infty}^{+\infty} R_x(\tau) e^{-i\omega t} dt \tag{2}$$

Where, $R_x(\tau)$ is the autocorrelation function of the signals.

Coherence function:

$$\gamma^2{}_{xy} = \frac{\left|S_{xy}(\omega)\right|^2}{S_x(\omega) S_y(\omega)} \tag{3}$$

The use of coherence function is similar to that of the correlation coefficients of time domain analysis. Coherence function represents the correlation between the signal output and the input signal. If the value of the coherence function is small, then it indicates that the output signal is greatly influenced by the external interference.

When analyzing a specific fault type of thin-walled robot bearings and selecting relevant parameters, it is necessary to analyze which variables are able to indicate the fault type and reflect the correlation between the fault type and the selected parameters. Generally, as long as the state of the bearing itself changes, all the relevant physical parameters will absolutely change accordingly. Thus, sensitivity and stability should be take into account when selecting the parameters in this paper. Based on the network structure of discussed, analyzing the time domain parameters can perfectly meet the needs of fault diagnosis. Therefore, apart from the aforementioned parameters, peak value X_{PEAK}, pulse index I, margin index *L*, kurtosis index K_{r} of vibration signals and peak-to-peak value $X_{\mathrm{p\text{-}p}}$, kurtosis index K_{r} of AE signals are also selected as state characteristics parameters. These parameters are represented as follows.

$$X_{\mathrm{PEAK}} = \frac{1}{n}\sum_{j=1}^{n} x_{pj} \tag{4}$$

$$X_{\mathrm{p\text{-}p}} = \max\{x_{\mathrm{n}}\} - \min\{x_{\mathrm{n}}\} \tag{5}$$

$$K_{\mathrm{r}} = N\sum_{\mathrm{n}=1}^{N} {x_{\mathrm{n}}}^{4} \Big/ {X^{4}}_{RMS} \tag{6}$$

$$I = X_{\mathrm{PEAK}} \Big/ \frac{1}{N}\sum_{\mathrm{n}=1}^{N} |x_{\mathrm{n}}| \tag{7}$$

$$L = X_{\mathrm{PEAK}} \Big/ \left(\frac{1}{N}\sum_{\mathrm{n}=1}^{N} \sqrt{|x_{\mathrm{n}}|}\right)^{2} \tag{8}$$

In the formulas, $\{x_{\mathrm{n}}\}(\mathrm{n}=1,2,...,\mathrm{N})$ represents signals, and N equals the number of sampling points. The signals are divided into n segments and $\{x_{pj}\}(j=1,2,...n)$ represent the peak value of those n segments.

3. Construction of SOM neural network and information integration

Neural network, also called as the connection model, is a mathematical algorithm created by imitating the neural network of the animal kingdom. It processes complex information by correlating the complex nodes that are similar to animal neurons within itself. Neural network needs to learn by certain rules before it can judge or fully describe things or information. Although neural networks have preliminary adaptive capabilities, the working efficiency and accuracy of neural networks can be greatly influenced by learning samples. So, if

the sample information is not comprehensive enough or contains some slight deviations, the working efficiency of the neural network will be greatly reduced.

SOM neural network has the self-organizing mapping ability. Therefore, it can model the competitive neural network of human brain system and has a strong classification characteristic for input vectors [25]. In the competition layer map, the input vector model of any dimension is transformed into discrete one-dimensional or two-dimensional graphics, which then achieve topological stability on the basis of the self-learning input vector model. Next, they are displayed in the competitive layer in the form classified as one-dimensional or two-dimensional through the autonomous learning of input vectors. Moreover, the probability distribution of the input model and the spatial distribution density of connection weights tend to be the same.

3.1 Network structure

As shown in Fig. 1, SOM network does not have a hidden layer while consists of only an input layer and a competitive layer. The upper layer of the network is a node matrix arranged by the output nodes (assuming the number of the output nodes is m) in a two-dimensional form while the input nodes located below. If the input vector consists of n elements, then the input port has a total of n nodes. All input nodes and output nodes are connected by weights. Specifically, in the two-dimensional plane, it is also possible that some output nodes are partially connected with each other. Based on the self-organizing method of Kohonen network, a large amount of sample training data is used to adjust the weight of the network in order to make the output of the final network be able to reflect the distribution of sample data.

The input layer consists of n one-dimensional neurons and each neuron is connected by weight. The competitive layer, namely the output layer, consists of a matrix of nodes whose quantity M equals m2. There are two kinds of weights in SOM, connection weight and characteristic weight. The former is the response of neurons to external inputs, and the latter determines the strength of the interaction between neurons.

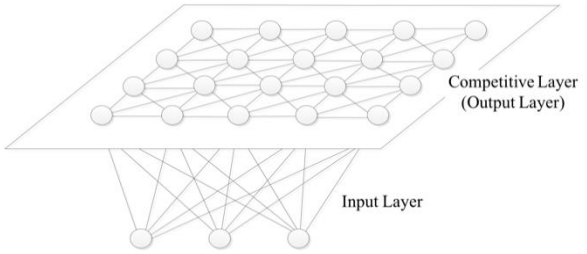

Fig. 1. Structure of SOM neural network

3.2 SOM neural network algorithm

When the network starts training, certain output node can make a special response to a certain pattern. When a certain type of data pattern is input, a certain output node is given the maximum stimulus to indicate the area where the pattern belongs to. And at the same time, some nodes around the winning node are given greater stimuli. When the input mode moves from one mode area to the neighboring mode area, the winning node on the two-dimensional plane also moves from the original node to its neighboring node. In order to make the neighboring output node in the two-dimensional output plane be able to make the special respond to the type of similar input patterns, the neighboring node of the winning node must be defined during the training process. Assuming that the winning point is Nj, and its neighboring node at the time t is represented by NEj(t), which contains all nodes falling into the circle whose center is the node Nj and the radius does not exceed a certain value. As the training process progresses, the radius of NEj(t) gets smaller and smaller, until the winning node Nj is the only node in the area. It means that in the initial stage of training, not only the weight of the winning node is adjusted, its geometrically neighboring nodes in a rather large range are also adjusted accordingly. Then, as the training process continues, the weight vector connected to the output node becomes closer and closer to the type of patterns it represents.

The specific algorithm flow is shown in Fig. 2:

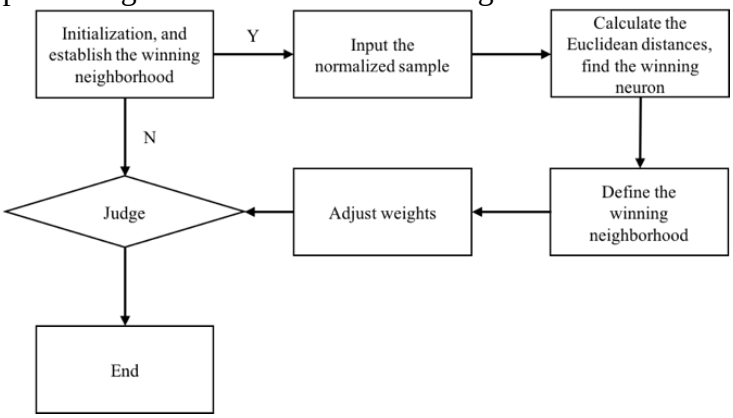

Fig. 2. Algorithmic flow of SOM neural network

The algorithm mainly contains the following steps: Firstly, a continuous input space of the active mode is produced according to a certain probability distribution, and an initial winning neighborhood is established, then an initial value is set for the learning rate. Secondly, a network topology is represented by a grid of neurons defines a discrete output space. Thirdly, a time-varying neighboring function is defined around the winning neuron. Finally, the learning rate parameter decreases by time but will never decrease to zero.

Following are the detailed steps of the algorithm.

(1) Initialization

Select a random value for the initial weight vector $w_j(0)$. The only limitation is that when $j=1,2,...,l$, each initial weight vector must be different with each other. l is the number of neurons in the network and needs to be kept at a rather small weight.

(2) Normalize samples

Normalize the input vector X of SOM network and each neuron vector $w_j(j=1,2,...,m)$ in the competitive layer and obtain $\hat{X}$ and $\hat{W}_j$.

$$\hat{X}=\frac{X}{\|X\|}\text{ , }\hat{W}_j=\frac{W_j}{\|W_j\|} \tag{9}$$

Vector $\hat{X}$ represents the active mode applied to the network and its number of dimensions equals m.

(3) Find the winning neuron

Compare the similarity between $\hat{X}$ and neuron vectors $\hat{W}_j$ $(j=1,2,...,m)$ in the competitive layer. The neuron of the highest similarity $i(x)$ wins.

$$i(x)=\arg\min\left\|x(n)-w_j\right\|,\ j=1,2,...,l \tag{10}$$

(4) Adjust weight

The winning neuron should be identified firstly, the output of the winning neuron is “1” and that of others are “0”.

$$y_i(t+1)=\begin{cases}1, j=j^*\\0, j\neq j^*\end{cases} \tag{11}$$

Only the winning neuron can adjust its weight vector W_{j^*}. Following is the learning adjustment of its weight vector.

$$w_j(n+1)=w_j(n)+\eta(n)h_{j,i(x)}(n)(x(n)-w_j(n)) \tag{12}$$

Adjust the weight vector of all neurons. $\eta(n)$ is the learning efficiency and its value range is $0<\eta(n)<1$. $h_{j,i(x)}(n)$ is the neighboring function of the winning neuron $i(x)$. For better results, $\eta(n)$ and $h_{j,i(x)}(n)$ change dynamically during the learning process. Learning efficiency decreases as the multi-dimensional learning progresses, which means the degree of adjustment becomes smaller and smaller and tends to the cluster center.

(5) Establish winning area

The normalized new vector must keep learning to re-normalize, establishing winning area and repeating the calculation cycle until the learning efficiency a decreases to zero.

3.3 Information integration

According to the data abstraction level, a multi-information integration system can be divided into three layers, namely, data layer fusion, feature layer fusion, and decision layer fusion. The multi-level information fusion model is shown in Fig. 3.

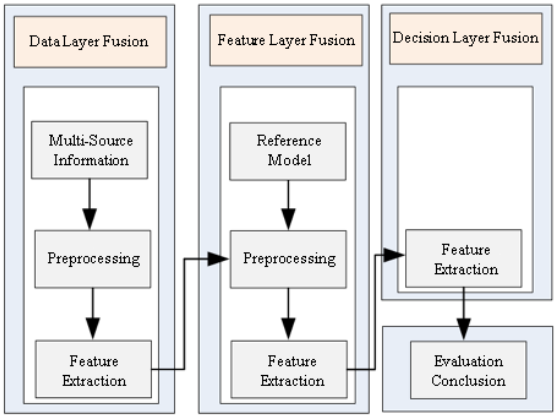

Fig. 3 Multi-level information fusion model

This paper uses the SOM neural network algorithm to construct a rolling bearing fault diagnosis method based on multi-sensor information fusion. The specific steps are as follows:

(1) Collect the vibration signals and AE signals of the robot bearing by using the vibration sensors and AE sensors placed in different positions, extract the characteristic parameters of the signals, and realize data layer fusion.

(2) Normalize the extracted characteristic parameters, fuse the two parameters and input them into SOM neural network as input vectors. Use the characteristic parameters to train SOM neural network, give the optimal weight vector W_j of SOM neural network and clustering centers, and achieve the fusion of feature layers.

(3) Based on the fusion of feature layers, input the corresponding test samples into the trained classifier to complete the extraction of characteristic parameters, realize the fusion of decision layers, and finally achieve the evaluation of the state of the robot bearing.

4. Robot bearing fault diagnosis experiment

Based on the aforementioned theories, this chapter takes robotic angular contact ball bearings ZR71820TN/P4 as an example to demonstrate a diagnosis experiment of its faults. The bearing material is GC15, the rolling body diameter is ϕ7.938 mm, the cage model is PA66-GF25 [26]. The main structural

parameters and technical specifications of the experimental bearing are shown in Table 1. And the built-up intelligent test bench for bearing performance is shown in Fig. 4.

Table 1

Structural parameters and technical specifications of bearings

Parameter	Value
External diameter/mm	125
Internal diameter/mm	100
Width/mm	13
Contact angle/ (°)	40
Number of rolling elements	38
Working speed/(r/min)	90
Rated dynamic load/kN	32.6

Fig. 4. Intelligent test bench for bearing performance

The vibration signal acquisition device is German m+p VibPilot-8 signal acquisition device. The vibration sensor is Lens LC0151T type acceleration sensor with a sensitivity of 146.2 mV/g and a range of 33g. The AE signal acquisition device and sensor are PCI-2AE collector and R50S-TCAE sensor, respectively. Their measurement range is from 50 kHz to 700 kHz and the resonant frequency is 500 kHz [27].

4.1 Experimental scheme and Network construction

YLP-MDF-152 type 3D fiber laser marking machine should be used to fabricate the three most typical fault states of the robot bearing's outer ring crack, inner ring crack and inner ring pitting corrosion, respectively. The widths of the outer ring crack and the inner ring crack are both 30 μm, and the diameter of the inner ring pitting is 50 μm. When the rotation speed is 80r/min and the equivalent

dynamic load is 7 kN, 4 sets of data were collected from the following four states, normal state, outer ring crack, inner ring crack, inner ring pitting, respectively, and a total of 16 sets of data were collected. Due to the limited size of the sample, the network structure was designed as 4x4, consisting of 16 neurons in total. The learning rate is 0.1. There are 500 training steps and 4 kinds of output states.

In the process of information fusion, considering the different physical meanings of signals collected by multi-sensor and the possibility of interfering SOM neural network, it is necessary to normalize the collected data [13]. Normalization can unify the physical quantities, avoid the possible no convergence caused by singular values impacting the network, and also increase the convergence speed of the network.

This paper uses formula (13) to normalize the collected data.

$$y = \frac{2 \times (x - x_{\min})}{y_{\max} - y_{\min}} - 1 \tag{13}$$

In the formula, x is raw data, y is normalized data with a range of [-1,1].

After normalizing the bearing's normal state, outer ring crack, inner ring crack, inner ring pitting, respectively, the results of the data normalization are shown in Table 2.

Table 2

Operation sample data of the bearing

Bearing state	Vibration data parameters					AE data parameters		
	RMS	C	Kr	I	L	RMS	PEAK	KR
Normal	-0.9892	0.9889	-0.9937	0.9822	0.9799	-0.5512	-0.9520	-0.9715
	-0.9911	0.4928	-1.0000	0.4849	0.4838	-0.5268	-1.0000	-1.0000
	-0.9960	0.6085	-0.9982	0.6031	0.6022	-0.4358	-0.9729	-0.9927
Outer race crack	0.7857	-0.1524	0.5574	-0.0546	0.0123	0.2016	-0.0089	-0.0728
	0.8707	-0.5172	0.5388	-0.5251	-0.5285	-0.0683	-0.1185	-0.0502
	0.8980	-0.7597	0.3053	-0.7614	-0.7631	0.2927	0.2914	0.7265
Inner race crack	1.0000	-1.0000	0.5575	-1.0000	-1.0000	-0.4374	-0.7815	-0.7789
	0.9859	-0.4638	0.5355	-0.4649	-0.4615	-0.4878	-0.7188	-0.7933
	0.9868	-0.7976	0.5732	-0.7904	-0.7832	0.1057	0.0914	0.0139
Inner race pitting	0.9906	-0.5951	0.2986	-0.5920	-0.5888	-1.0000	-0.8612	0.3554
	0.9552	-0.4816	0.5347	-0.4404	-0.4123	-0.9008	-0.6355	0.8501
	0.9664	-0.4883	1.0000	-0.4783	-0.4704	-0.8813	-0.9087	-0.5226

The data in Table 2 is input into the neural network for training. The input vector model, designed as $^{12\times8}$, consists of 12 sets of data and 8 parameters. After 500 training steps in the network, the distribution of weight vectors is shown in Fig. 5, and the weight no longer changes (The software tools used in this paper is Matlab).

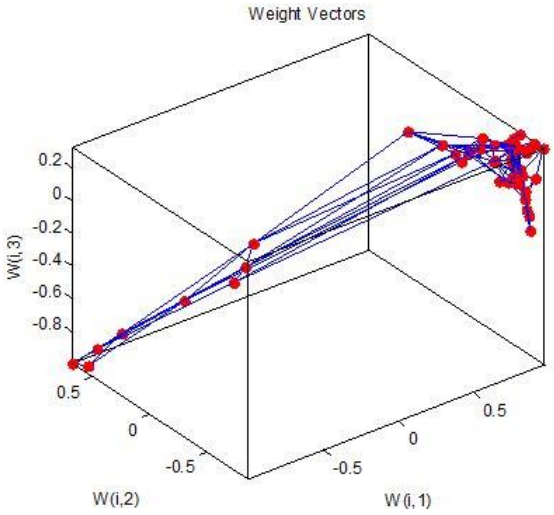

Fig. 5. Distribution of weight vectors

Fig. 6 shows the Euclidean distances between neurons after training. For each neuron, the darker surrounding color and the greater distance mean the lower probability of "winning", while the neuron whose surrounding color is lighter has a greater possibility of "winning". Then, the connection weight of the winning neuron represents the cluster center of the state. Later, whenever a test sample is input, the network will automatically match it with the previously classified sample.

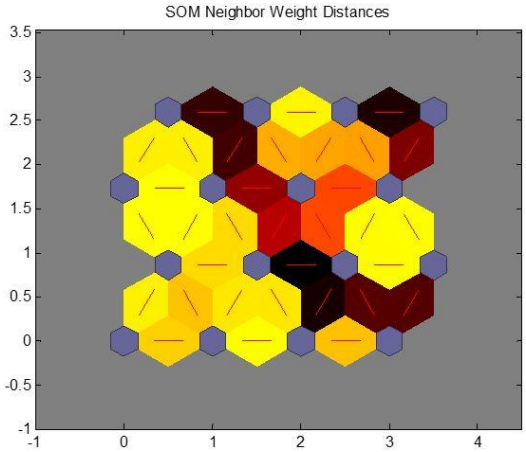

Fig. 6. The distances between neurons

Fig. 7 shows the classification of the trained data by the network. Each of the four neurons of darker color shows the number of input vectors it classifies, and the relative number of each neuron is indicated by the size of the color stain.

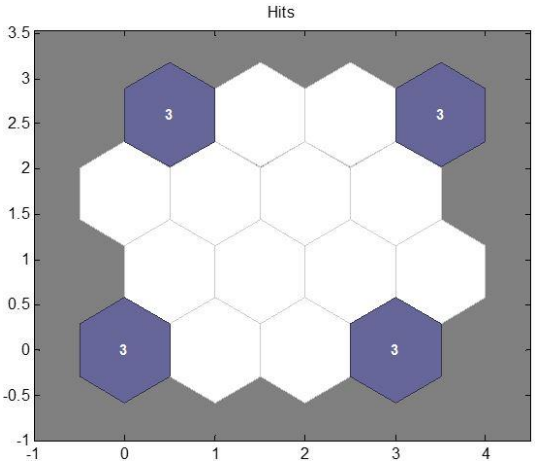

Fig. 7. The classification of input vectors by neurons

According to Fig. 6, the 12 sets of data of the operated sample are divided into 4 categories by SOM neural network and each category contains 3 input vectors.

4.2 Experimental predictions

After the training, first set up a test sample data (Table 3) to test the diagnostic effect of SOM neural network.

Table 3

Test sample data for bearing

Bearing state	Vibration data parameters					AE data parameters		
	RMS	C	Kr	I	L	RMS	PEAK	KR
Normal	-1.0000	1.0000	-0.9978	1.0000	1.0000	-0.4650	-0.9834	-0.9854
Outer race crack	0.9009	-0.5373	0.0290	-0.5251	-0.5173	0.2049	0.2024	0.4410
Inner race	0.9818	-0.4705	0.4134	-0.4582	-0.4458	1.0000	1.0000	1.0000
Inner race pitting	0.967	-0.8977	0.6765	-0.8751	-0.8570	-0.9024	-0.9487	-0.5247

As shown in Fig. 8 (a), the bearing states are indicated by number from 1 to 16. Specifically, number 1 to 4, 5 to 8, 9 to 12, and 13 to 16 refer to normal state, inner ring crack, inner ring pitting, and outer ring crack, respectively. When a test sample is classified, its state can be easily determined by simply activating the winning neuron and entering its neighborhood.

The data model is designed as 4x8. Fig. 8 (b) shows the classification results after inputting the trained SOM neural network.

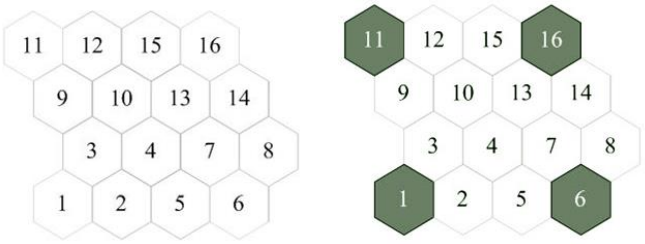

(a) (b)

Fig. 8. The results of state classification

According to Fig. 8, the test sample's normal state, inner ring crack state, inner ring pitting state, and outer ring crack state coincide with those were indicated as "1", "6", "11", and "16" in the running sample. The output results are ideal since all four states are correctly determined.

5. Conclusions

The results of inputting the data integrated by vibration data and AE data as input vectors into SOM neural network indicate the validity of the fault diagnosis of robot bearings based on information-integrated SOM neural network. This method not only makes full use of SOM neural network's advantage of reducing dimensions, but also proves the feasibility of combining dimensional parameters and dimensionless parameters as input vectors when conducting time domain analyses. Therefore, it can be concluded that this method has a practical application value in the fault diagnosis of robot bearings.

Acknowledgements

Thanks to Henan University of Science and Technology for the experiments.

R E F E R E N C E S

[1]. *S. Cai, Y. Chen, J. Ye, and L. Sun*, Design and analysis of thin wall sealed bearing structure for industrial robot. Bearing, **vol.** 12, 2007, pp. 10-13.

[2]. *X. Wang, Y. Liu, F. Cui, and Z. Zhang*, Self-positioning Analysis of Thin-Walled Bearing Rings in Rotating Gas Field. Journal of Henan University of Science and Technology: Natural Science, **vol.** 34, no. 3, 2013, pp. 21-25.

[3]. *Y. Jiang, Y. Wang, K. Zhao, and D. Su*, Mechanical Property Analysis of Flexible Thin Bearing in Harmonic Drive. Bearing, **vol.** 1, 2017, pp. 10-14.

[4]. *Y. Jia, Q. Shan, J. Li, and F. Kang*, Application of Semi-Automatic Quenching Press in Distortion Control of Thin-Walled Bearing Rings. Bearing, **vol.** 2, 2016, pp. 24-26.

[5]. *N. P. Kashif, Z. A. Azzedine*, Newton-like Algorithm for Adaptive Multi-Modulus Blind Equalization. 7th International Workshop on Systems, Signal Processing and Their Applications (WOSSPA), 2011, pp. 283-286.

[6]. *W. Ostapski, I. Mukha,* Stress State Analysis of Harmonic Drive Elements by FEM. Technical Sciences, **vol.** 1, 2007, pp. 115-123.
[7]. *W. Ostapski,* Analysis of the Stress State in the Harmonic Drive Generator Flex Spline System in Relation to Selected Structural Parameters and Manufacturing Deviations. Bulletin of the Polish Academy of Sciences Technical Sciences, **vol.** 4, 2010, pp. 693-698.
[8]. *W. Sui,* Investigation on Feature Extraction and Diagnosis Method of Surface Damage Faults of Rolling Bearings. Shandong University, 2011.
[9]. *F. Deng,* Research on Fault Feature Extraction and Diagnosis Method of Rolling Element Bearing. North China Electric Power University, 2016.
[10]. *B. He,* Investigation on bearing fault identification and performance degradation assessment based on KJADE. Anhui University, 2017.
[11]. *K. Xue,* Research on Feature Recognition Method of Common Faults of Aero-engine AE Signal Based on Rough Set. Beijing University of Chemical Technology, 2017.
[12]. *Y. Jiang,* Research on Aero-engine Bearing Fault Diagnosis Based on Texture Feature. Beijing University of Chemical Technology, 2017.
[13]. *C. Wang,* Mechanical signal processing based on sparse representation and its application in the diagnosis of rolling-element bearings. University of Science and Technology of China, 2017.
[14]. *J. Hen, D. Yu, Y. Yang,* A fault diagnosis approach for roller bearings based on EMD method and AR model. Mechanical Systems and Signal Processing, **vol.** 20, no. 2, 2006, pp. 350-362.
[15]. *H. Qiu, J. Lee, J. Lin, et a1.,* Wavelet filter-based weak signature detection method and its application on rolling element bearing prognostics. Journal of Sound 106 and Vibration, **vol.** 289, 2006, 1066-1090.
[16]. *R. Kumar, M. Singh,* Outer race defect width measurement in taper roller bearing using discrete wavelet transform of vibration signal. Measurement, **vol.** 46, 2013, pp. 537-545.
[17]. *B. Han,* Research on Multi-Sensor Information Fusion Fault Diagnosis Method based on AR-SVPMCD. Southeast University, 2015.
[18]. *R. Li,* Research on Multi-Sensor Bearing Fault Diagnosis Based on GA-BP Neural Network. Control and Instruments in Chemical Industry, **vol.** 44, no. 10, 2017, pp. 916-920.
[19]. *Y. Han,* Rolling Bearing Fault Diagnosis Based on Multi Sensor. Henan University of Science and Technology, 2015.
[20]. *K. Yu,* Fault Diagnosis of Rolling Element Bearings Based on Deep Belief Network and Multiple Sensors Information Fusion. Qingdao University of Technology, 2016.
[21]. *N. Tando., B. C. Nakra,* Defect detection of rollillg element beatings by acoustic emission method. Journal of acoustic emission, **vol.** 9, no. 1, 1990, pp. 25-28.
[22]. *A. Choundhury, and N. Tandon,* Application of acoustic emission technique for the detection of defects in rollillg element bearings.Tribology, international, **vol.** 33, 2000, pp. 39-45.
[23]. *Y. H. Liu, Z. W. Yu, M. Zeng, et a1.,* An improved LLE algorithm based on iterative shrinkage for machinery fault diagnosis. Measurement, **vol.** 77, 2016, pp. 246-256.
[24]. *X. Wang, J. Yang, Y. Guo,* Probability Theory and Mathematical Statistics. Beijing University of posts and telecommunications press, 2017.
[25]. *Y. S. Li,* Mathematical modelling and characteristics of the pilot valve applied to a jet-pipe/deflector-jet servovalve, Sensors and Actuators A, **vol.** 245, 2016, pp. 150-159.
[26]. Retainer of non-standard thin-walled angular contact ball bearing, https://patents.google.com/patent/CN201982512U/en.
[27]. LC0151T type acceleration sensor and R50S-TCAE sensor, http://www.lance-sensor.com/product/lc01.htm.